GNSS Absolute Antenna Calibration at the National Geodetic Survey

Andria Bilich, Gerald L. Mader, *National Geodetic Survey*

BIOGRAPHY

Andria Bilich received the B.S. degree in geophysics from the University of Texas, Austin, in 1999, and the Ph.D. degree in aerospace engineering sciences from the University of Colorado, Boulder, in 2006. Dr. Bilich is a Geodesist with the National Geodetic Survey – Geosciences Research Division. Her research interests include GPS multipath characterization, GNSS antenna calibration, and precision improvements to GNSS positioning for geoscience applications.

Gerald Mader is Chief of the Geosciences Division of the National Geodetic Survey where he has worked since 1983. Dr. Mader received a B.A. in Physics from Rutgers in 1969 and a Ph.D. in Astronomy from the University of Maryland in 1975. He has developed techniques and programs for precise static and kinematic GPS positioning and for NGS' antenna calibration program.

ABSTRACT

To help meet the needs of the high-precision GNSS community, the National Geodetic Survey (NGS) will soon begin operations of an absolute antenna calibration facility. Located in Corbin, Virginia, this facility uses field measurements and actual GNSS satellite signals to quantitatively determine the carrier phase advance/delay introduced by the antenna element.

In this paper we describe the NGS calibration facility and provide the time-difference, single-difference carrier phase observable models and estimation strategy currently used to generate NGS absolute calibrations. Examples of antenna calibrations from the NGS facility provide context for the discussion, and demonstrate that NGS phase center variations (PCVs) agree within 1 mm with other calibration techniques. Finally, user-friendly features of the revamped NGS Calibration Services are discussed.

INTRODUCTION

Many GNSS applications now routinely demand millimeter precision and extremely high levels of accuracy. To achieve these accuracies, measurement and instrument biases at the centimeter to millimeter level must be understood. One of these biases is the antenna phase center (APC), a theoretical point of GNSS signal reception for an antenna. The APC is not a single point, but depends upon the direction of signal reception.

The antenna phase center is most often described by two quantities, the mean phase center or phase center offset (PCO) plus phase center variations (PCVs). Both PCOs and PCVs are direction dependent and defined in an antenna-fixed reference frame. The antenna frame origin is the antenna reference point (ARP), typically the center of the antenna base at the attachment point. The frame orientation is typically defined by a North reference mark on the antenna. PCOs are normally described as north-east-up offsets from the ARP. PCVs depend upon the direction of signal reception, and are described as a function of elevation angle and azimuth angle. Together PCO and PCV for a single antenna provide a complete description of the phase delay or advance introduced to the incoming signal by the antenna elements. Furthermore, APC depends on the frequency of the incoming signal, thus each GNSS signal requires its own calibration.

The APC (PCO + PCV) of an antenna can be measured to create a calibration for that antenna. For over 15 years, the National Geodetic Survey (NGS) has computed relative calibrations. In a relative calibration, the antenna to be calibrated (test antenna) is placed on a pillar, on a short baseline adjacent to a reference antenna. Phase data are collected over 24 hours, and used to determine the test antenna's APC relative to the reference antenna [1]. These relative calibrations ignored azimuth effects because azimuthal variations are quite small for the majority of geodetic antennas. The distribution of relative calibration data was at the mercy of available satellite

23rd International Technical Meeting of the Satellite Division of
The Institute of Navigation, Portland, OR, September 21-24, 2010

coverage, which was often sparse, especially near the zenith. In addition, the assumptions of relative calibrations broke down over long baselines where earth curvature caused the same satellite to be viewed at significantly different elevation angles.

To correct these shortcomings, the geodetic community has moved to absolute calibrations, where the resultant calibration is independent of the reference antenna. Absolute calibrations are routinely computed by several institutions implementing different methods. For example, Geo++ conducts field calibrations with signals from all GNSS satellites in view (multiple transmitting antennas) and uses a 3-axis robot to move the test antenna [2]. In contrast, Technische Universitat Darmstadt conducts anechoic chamber calibrations using a 2-axis robot, a signal analyzer, and a single transmitting antenna. Despite the methodological differences, these methods show very close agreement [3].

Phase center calibrations are proving to be an important factor in high precision GNSS positioning [4, 5]. For example, permanent geodetic networks exist all over the globe but use a mix of antennas; applying calibrations at the processing level brings all the phase centers into agreement. Similarly, if identical antennas were used on a very long (> 1000 km) baseline, the same satellite would be received at different angles and experience different phase center advance/delay factors; phase center calibrations applied to the phase observables would remove this long baseline effect.

For both relative and absolute calibration systems, the APC for all serial numbers of antenna within a manufacturer's model run are typically consistent with each other, and can thus be described by a type mean value [2]. The International GNSS Service (IGS) maintains a database of type mean calibrations for antennas used at IGS network stations. Some antennas may deviate strongly from the type mean. In those cases, an individual calibration must be performed. It has been well established that phase center patterns differ between antenna models and manufacturers [1]; additional research suggests that the addition of a radome or the choice of antenna mount can significantly alter those a priori phase center patterns [6, 7]. Thus it is important to generate type mean calibrations for new antenna models entering the market, and to conduct individual calibrations for non-standard antenna installations or antennas which appear to deviate from the type mean.

In this paper we describe NGS's recently-developed absolute antenna calibration facility. After describing the salient features of the calibration facility itself, the observation equations are sequentially described so that the reader can understand the reasoning behind "absolute" calibration. To demonstrate the accuracy of this calibration method, we compare some sample NGS results to the published IGS type mean values.

CALIBRATION FACILITY

The NGS absolute calibration facility consists of two antennas on a very short (5 m) baseline. The reference and test XYZ monument positions were first determined via a combination of NGS OPUS-Static and single-frequency solutions on a short baseline. The relative accuracy of these XYZ positions was further refined by placing absolutely calibrated antennas on each end of the baseline. After removing the known PCVs and other pre-determined geometric factors (described below), we verified that the residual double-difference phase observable combination has a constant mean over a satellite pass.

The calibration baseline is situated in a large, flat field with no significant sky obstructions and only a few reflecting objects in the farfield (Fig. 1). Extensive multipath testing has been conducted to prove that the dominant multipath sources are ground reflections.

Data are recorded using a Septentrio AsteRx2eH GNSS heading receiver. This receiver is intended to track signals from several antennas on an aircraft, and thus has multiple antenna inputs with a common clock to track signals from all antennas. In this application, the heading receiver is connected to both the test and reference antennas. The common clock allows easy removal of receiver clock biases when forming the short-baseline observable combinations for antenna calibration.

As will be discussed below, angles of signal reception must be rapidly changed during calibration, thus the antenna under test must be moved through a large range of motions. We accomplish test antenna motion using a robot. The current facility uses a Directed Perception pan-tilt unit (PTU), model PTU-D300 (Fig. 2). This 2-axis robot is capable of pan motions (rotations about a vertical axis aligned with local up) as well as tilt motions around one horizontal axis.

Figure 1: Absolute antenna calibration baseline, located at NGS facility in Corbin, VA.

Figure 2: Two-axis robot used to move the antenna under test, shown here with a Trimble Zephyr Geodetic II antenna and 20-cm extension to separate antenna from the robot body.

Moving the test antenna has additional benefits. First, by moving the antenna through a full range of pan and tilt motions, signals are received at all possible angles (Fig. 3). If the antenna remained fixed, only certain signal paths would be sampled, and it would be impossible to achieve the required data density to solve for PCV with respect to azimuth as well as elevation angle. Also, moving the antenna allows us to maintain a high local elevation angle mask while still sampling the entire pattern of interest. In this study, data below 15 degrees in the local reference frame are removed from analysis. Additionally, an antenna frame elevation cutoff of -5 degrees is applied.

OBSERVABLE COMBINATION

To prepare raw carrier phase data for phase center estimation, several known factors and biases must be addressed (see following section on *a priori* models). After removing or accounting for these factors, the initial phase residuals ϕ for the reference antenna (subscript *ref*) and antenna under test (subscript *test*) for a single satellite *sv* are:

$$\phi_{ref}^{sv} = \delta_{rx} - \delta^{sv} + A + MP_{ref} + APC_{ref} + N_{ref} + \varepsilon_{ref} \quad (1)$$

$$\phi_{test}^{sv} = \delta_{rx} + DHB - \delta^{sv} + A + MP_{test} + APC_{test} + N_{test} + \varepsilon_{test} \quad (2)$$

These equations have terms for the respective antenna phase centers *APC*, as well as integer ambiguity *N*, phase noise ε and phase multipath *MP* for each antenna. Note the common terms for the receiver clock δ_{rx}, satellite clock δ^{sv}, and atmospheric parameters *A* (troposphere, ionosphere). The common receiver clock term results from the use of a dual-antenna receiver, however the same equations hold true for separate receivers driven by an external clock. Note that even with a common clock, a differential hardware bias *DHB* will exist in the system; we assign DHB to the test antenna, even though it is differential between the test and reference channels. Due to the very short baseline (5m), a satellite signal will travel a nearly identical atmospheric path before reception by either antenna. Therefore atmospheric parameters such as troposphere and ionosphere are considered equivalent for each antenna. Some random phase noise ε is expected for real observations. Forming the between-receiver single difference (two stations, single satellite) of these phase residuals removes atmospheric effects as well as both satellite and receiver clock terms:

$$\Delta\phi = \phi_{test}^{sv} - \phi_{ref}^{sv} = APC_{test} - APC_{ref} + DHB + MP_{test} - MP_{ref} + \Delta N + \Delta\varepsilon \quad (3)$$

After forming the single difference phase combination, data are edited for cycle slips and the single-difference ambiguities are removed.

Before going further, the APC should be defined more explicitly for a specific satellite. Written in terms of the advancing or delaying effects on the carrier phase observable, APC is the projection of the PCO vector onto the satellite line-of-sight *LOS* plus phase center variations. Like the line-of-sight vector, PCVs are also a function of the elevation θ and azimuth α angles of reception in the antenna fixed frame, therefore:

$$APC = \overrightarrow{PCO} \cdot \overrightarrow{LOS}(\theta, \alpha) + PCV(\theta, \alpha) \quad (4)$$

To effectively estimate PCO and PCVs, all factors except phase center at the test antenna must be removed from the observable. Furthermore, an *absolute* antenna calibration is only possible if the reference antenna phase center is properly negated. We accomplish this by collecting data from two different test antenna orientations, where the different antenna orientations are closely spaced in time (< 10 seconds). We expand Eq. 3 for times A and B while also incorporating Eq. 4:

$$\Delta\phi_A = \overrightarrow{PCO}_{test} \cdot \overrightarrow{LOS}(\theta_A, \alpha_A) + PCV_{test}(\theta_A, \alpha_A) - \left(\overrightarrow{PCO}_{ref} \cdot \overrightarrow{LOS}(\theta, \alpha) + PCV_{ref}(\theta, \alpha)\right) + DHB_A + MP_{test}(\theta_A) - MP_{ref}(\theta) + \Delta\varepsilon_A \quad (5)$$

$$\Delta\phi_B = \overrightarrow{PCO}_{test} \cdot \overrightarrow{LOS}(\theta_B, \alpha_B) + PCV_{test}(\theta_B, \alpha_B) - \left(\overrightarrow{PCO}_{ref} \cdot \overrightarrow{LOS}(\theta, \alpha) + PCV_{ref}(\theta, \alpha)\right) + DHB_B + MP_{test}(\theta_B) - MP_{ref}(\theta) + \Delta\varepsilon_B \quad (6)$$

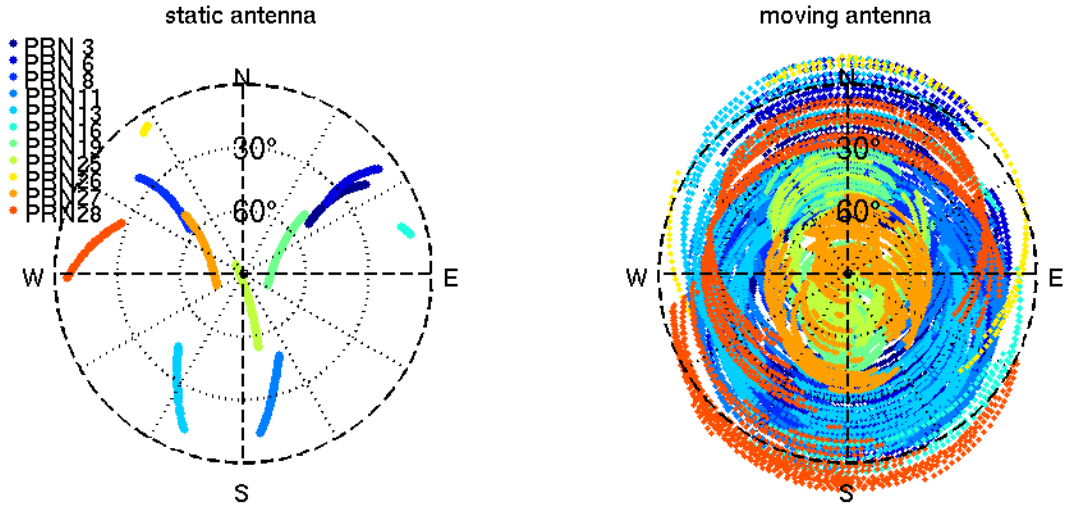

Figure 3: Polar plots showing azimuth and elevation angles of GPS signal reception over 2 hours for a fixed antenna (left) versus a moving antenna (right) which moves through [-180,180] deg of pan and [-25,30] deg of tilt. Colors correspond to GPS PRN numbers.

Satellite motion in the local ENU frame is negligible for closely-spaced times A and B. In our calibration scenario the reference antenna remains fixed, thus from the perspective of the reference antenna the angles of reception (θ, α without subscripts) do not change between A and B. However, between A and B the test antenna undergoes significant motion, so that $\theta_A \neq \theta_B$ and $\alpha_A \neq \alpha_B$. Forming the time difference of single difference (TDSD) observable removes phase center and multipath error at the reference antenna:

$$\begin{aligned}\mathrm{TDSD_{AB}} = \;& \Delta\phi_A - \Delta\phi_B \\ \mathrm{TDSD_{AB}} = \;& \overrightarrow{PCO}_{test} \cdot \overrightarrow{LOS}(\theta_A, \alpha_A) \\ & + PCV_{test}(\theta_A, \alpha_A) \\ & - \left(\overrightarrow{PCO}_{test} \cdot \overrightarrow{LOS}(\theta_B, \alpha_B)\right. \\ & \left. + PCV_{test}(\theta_B, \alpha_B)\right) \\ & + MP_{test}(\theta_A) - MP_{test}(\theta_B) \\ & + \Delta DHB_{\mathrm{AB}} + \Delta\Delta\varepsilon_{\mathrm{AB}}\end{aligned} \quad (7)$$

Additional simplifications can be safely made. First, for the Septentrio AsteRx2eH and the hardware configuration at the Corbin calibration facility, differential hardware bias varies slowly in time (~ 0.1 cycles of drift over 1 hour), rendering ΔDHB_{AB} negligible over the short time span between times A and B. Second, antenna motions are programmed so that the PTU will change its azimuth (pan) between times A and B, resulting in TDSD time pairs where the antenna is a fixed height above the ground. The standard multipath ray tracing approximation [8] dictates that the differential multipath error for an antenna at a fixed distance from a reflecting object will also be negligible. Therefore, all multipath from the ground (the primary reflecting surface) is differentially eliminated and all remaining multipath from isolated farfield objects is averaged out. The final TDSD contains only phase center terms for the antenna under test plus differential phase noise:

$$\begin{aligned}\mathrm{TDSD_{AB}} = \;& \overrightarrow{PCO}_{test} \cdot \overrightarrow{LOS}(\theta_A, \alpha_A) \\ & + PCV_{test}(\theta_A, \alpha_A) \\ & - \left(\overrightarrow{PCO}_{test} \cdot \overrightarrow{LOS}(\theta_B, \alpha_B)\right. \\ & \left. + PCV_{test}(\theta_B, \alpha_B)\right) \\ & + \Delta\Delta\varepsilon_{\mathrm{AB}}\end{aligned} \quad (8)$$

Preliminary sensitivity testing supports our assertions about the observable combinations. Although not shown here, we have verified TDSD independence from reference antenna effects by conducting calibration runs with different reference antennas. For these tests, the final PCO and PCV values differ at the sub-mm level. We have also conducted preliminary simulations of expected multipath errors. Using the simple ray tracing formulation of carrier phase multipath errors [8] and examples of various geodetic antenna gain patterns, our simulations show that TDSD with pan-only motions will result in negligible and zero-mean multipath errors in the TDSD observable.

A PRIORI MODELS

As mentioned above, a number of factors must be accounted for, or modeled and removed from the observable, to yield the initial phase residuals from Eq. 1 and 2. Those factors are: geometric range between monument XYZ and satellite; frame alignment (robot reference frame vs. local ENU); time system offset between antenna motions and GPS observations; measurement of PTU rotation arm, and projection of that

arm onto satellite line-of-sight; phase windup for moving antenna.

Satellite orbits are required to compute and remove geometric range from the raw carrier phase observable, as well as calculate azimuth and elevation angles in the local ENU frame. We use the GPS standard broadcast navigation message to compute satellite orbits. Sensitivity tests show no appreciable gains from using more precise satellite products, which is expected given that the single-difference phase (Eq. 3) should also remove common orbit biases.

PTU motions are controlled by the data collection PC, and those motions must be directly related to GPS time for synchronization with the phase observations. Unfortunately, most PC clocks are poor quality, with a large unknown bias from GPS time plus a significant drift. We implemented the NIST Time freeware (http://www.nist.gov/physlab/div847/grp40/its.cfm) to synchronize the PC clock to the NIST time server. Our implementation of the NIST software synchronizes the PC clock every hour and sufficiently corrects for clock drift to maintain PC-UTC synchronization to << 0.2 seconds.

Differential leveling of the calibration setup yielded a PTU rotation point to top of payload bracket distance of 0.1187 m. Furthermore, a 10-cm or 20-cm extension (Fig. 2) is added to mitigate any possible antenna-robot electromagnetic coupling which might affect the APC. With extensions, the full PTU rotation to antenna reference point (ARP) distance becomes 0.2187 m or 0.3187 m. Because these values are close to or larger than a full GPS wavelength, careful attention must be taken during cycle slip detection and editing.

The precise orientation of the PTU relative to the local east-north-up (ENU) frame must be well-determined for correct determination of angles of signal reception in the test antenna body frame. The PTU is leveled so that its horizontal frame is parallel to the local east-north plane, and the PTU tilt plane is precisely aligned with the north pier. The south-north pier azimuth was measured as 1.40 deg counter-clockwise from true north via GPS position solutions and transformation with NGS INVERS3D (http://www.ngs.noaa.gov/TOOLS/Inv_Fwd/Inv_Fwd.html).

Because the test antenna undergoes significant rotations relative to the satellite frame, phase windup must also be removed. Although phase windup effects are small (< 0.1 cycles), they are significant for the mm-level phase residuals required for APC solution. We implemented the phase windup model of [9] to remove phase windup when editing the carrier phase observables.

SOLUTION METHOD AND REPRESENTATION

To calibrate an antenna, the TDSD observables (Eq. 8) are formed for a large number of time AB combinations, then passed to a 2-stage least squares solution routine. First, we solve for the mean phase center (PCO) by temporarily ignoring variations due to the PCVs:

$$\begin{aligned} \mathrm{TDSD}_{AB} = & \quad \overrightarrow{PCO}_{test} \cdot \overrightarrow{LOS}(\theta_A, \alpha_A) \\ & - \overrightarrow{PCO}_{test} \cdot \overrightarrow{LOS}(\theta_B, \alpha_B) \\ = & \quad \overrightarrow{PCO}_{test} \cdot \left(\overrightarrow{LOS}(\theta_A, \alpha_A) - \overrightarrow{LOS}(\theta_B, \alpha_B) \right) \end{aligned} \tag{9}$$

For the second estimation stage, the PCO solution $\widehat{PCO}$ must be removed from the TDSD observations. The derivative ΔTDSD observable captures the PCVs over two sets of angles:

$$\begin{aligned} \Delta TDSD_{AB} = & \quad TDSD_{AB} - \\ & \widehat{PCO} \cdot \left(\overrightarrow{LOS}(\theta_A, \alpha_A) \right. \\ & \left. - \overrightarrow{LOS}(\theta_B, \alpha_B) \right) \\ = & \quad PCV_{test}(\theta_A, \alpha_A) - PCV_{test}(\theta_B, \alpha_B) \end{aligned} \tag{10}$$

The two-stage approach is required because we solve for PCVs using surface spherical harmonics. Eq. 10 can be written as the difference of two surface spherical harmonic expansions, i.e. the expansion for θ_A, α_A minus the expansion around θ_B, α_B. The differential nature of ΔTDSD means that the zero degree surface spherical harmonic is differenced away when forming the design matrix, thus the zero degree harmonic cannot be accessed. Independently solving for PCO avoids this pitfall and results in a robust inversion for surface spherical harmonic coefficients.

Two different surface spherical harmonic expansions are used to solve for two different representations of PCV. First, a degree 8 order 0 expansion is used to capture PCV as a function of only elevation angle. This representation is necessary because many GNSS analysis software can only accept elevation-only specifications of PCVs. This simplified PCV representation shows the gross features of spatial dependence; to capture the full range of azimuthal dependence, we use the same ΔTDSD to estimate coefficients to a degree 8 order 5 spherical harmonic expansion.

ABSOLUTE CALIBRATION EXAMPLES

NGS absolute calibrations must be directly compatible with published IGS values, to facilitate combination of our calibration values with those of other institutions. Thus in the following examples we compare NGS solutions to IGS05 ANTEX values (ftp://igscb.jpl.nasa.gov/igscb/station/general/igs05.atx; note that the IGS will soon issue IGS08 standards and

products, so this link may change) as a truth standard. The IGS05 values are type means, where 2-20 different serial numbers from within a model group are individually calibrated, and their PCO/PCV solutions are combined to create a mean APC for the antenna model. The examples in this section compare individual calibrations to type means, so a moderate level of discrepancies between NGS and IGS values is expected.

The accepted standard for comparing calibrations from different institutions is to use a common PCO value for both. Because APC = PCO + PCV, comparison with common PCO requires a geometric transformation of one party's PCV pattern. All of the following PCV results are after shifting NGS PCVs into agreement with the respective IGS PCO.

Trimble Zephyr Geodetic 2 (TRM55971.00)

We computed individual calibrations for two different serial numbers of Trimble Zephyr Geodetic 2 antennas, S/N 30212661 and 30212716. The resulting PCOs (Table 1) differ from IGS by almost 2 mm in the vertical component, but the horizontal components are nearly identical. Fig. 4 provides the elevation-only PCVs as a function of elevation angle in the antenna frame. Note that, as with all PCV solutions shown in this paper, NGS PCV values have already been transformed to use the IGS PCO value (e.g. for the Zephyr Geodetic II, PCO = [1.07 -0.19 67.17] mm).

Fig. 5a depicts the full PCV solutions from NGS calibrations. This style of plot represents the dependence of PCVs on both the elevation and azimuth. The center of the plot is the antenna boresight (90 deg elevation), whereas the outside edge is the antenna horizon (0 deg elevation). The top of each circle is equivalent to North in the antenna frame. The PCVs for the calibrated Zephyr Geodetic II antennas appear as concentric circles (except at the very lowest elevation angles), meaning that the PCVs have very little azimuthal dependence. The full PCVs show sub-mm differences from the published IGS type mean (Fig. 5b).

Ashtech Geodetic III "Whopper" (ASH700718B)

We also computed individual calibrations for two different serial numbers of Ashtech Geodetic III "Whopper" antennas, S/N 11885 and 11869. The resulting PCO values differ from IGS at the sub-mm level in all components (Table 2). Viewing PCVs using the elevation-only pattern (Fig. 6), the NGS values again have sub-mm agreement with the IGS type mean, and differ from each other by at most ~ 0.5 mm over the elevation angle range shown. Differences amongst individual calibrations (serial numbers) within a model group seldom exceed 1-2 mm - this is considered sufficient to publish a type mean value where individual calibrations are averaged to create a mean value for the model group.

The complexities of this antenna's PCVs are most apparent when azimuthal variations are brought into view (Fig. 7). The Whopper antenna has 4 distinct lobes, two with maxima of 5 mm and two with minima of -6 mm. This strong azimuthal dependence emphasizes the importance of PCVs. For example, a satellite at 20 deg elevation angle observed to the south would experience about -7 mm of L1 phase delay, whereas a different satellite observed to the east at the same elevation would experience 4 mm of L1 phase advance – a net difference of 1.1 cm with sole dependence upon satellite azimuth. Deviations of the NGS individual calibrations from the IGS type mean are at the < 1mm level for most of the pattern, but the lobe maxima/minima or horizon values can differ by up to 2.5 mm. This level of discrepancy is not surprising given that we are comparing individual and type mean calibrations for a highly variable antenna pattern.

Table 1: NGS PCO solution for two different serial numbers of Trimble Zephyr Geodetic 2 antennas, compared to IGS05 type mean values.

(mm)	North	East	Up
IGS	1.07	-0.19	67.17
30212661	1.38	-0.45	69.84
30212716	0.92	-0.47	69.84

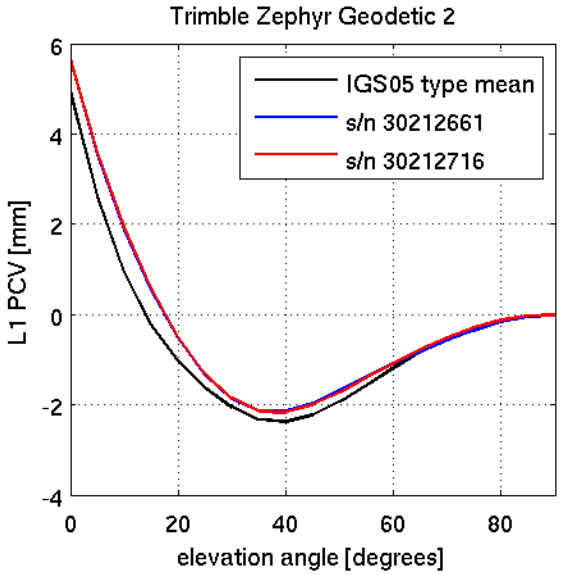

Figure 4: Elevation-only PCVs, GPS L1 frequency, for the Trimble Zephyr Geodetic II antenna. The two serial numbers calibrated (30212661, 30212716) show sub-mm agreement with the IGS type mean for this antenna.

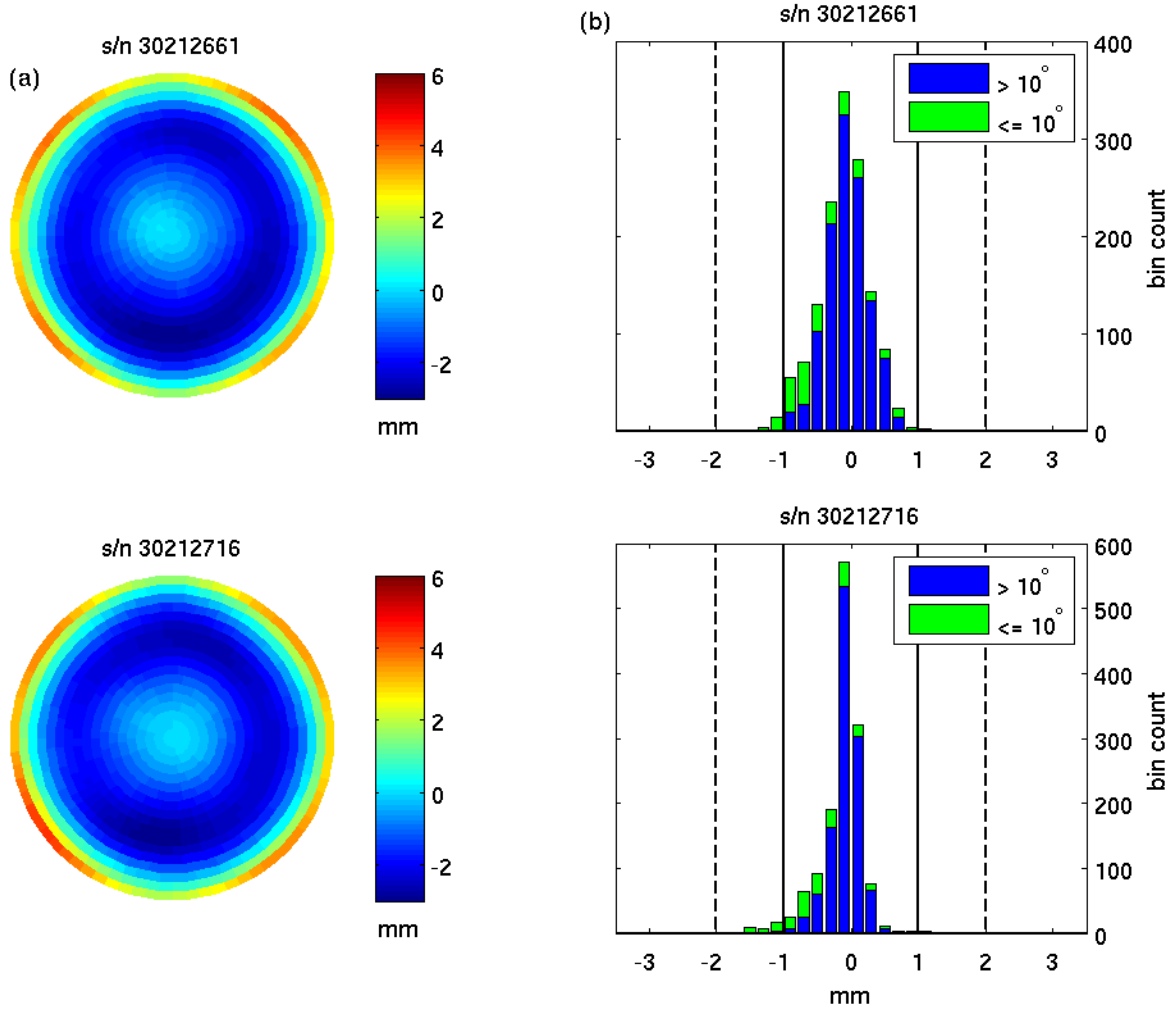

Figure 5: (a) L1 PCVs for the individual calibrations of two Trimble Zephyr Geodetic II antennas as a function of azimuth and elevation angle. The color scale is in mm. (b) Differences of NGS PCVs from IGS type mean, provided for elevation angles above 10 deg (blue) and below 10 deg (green).

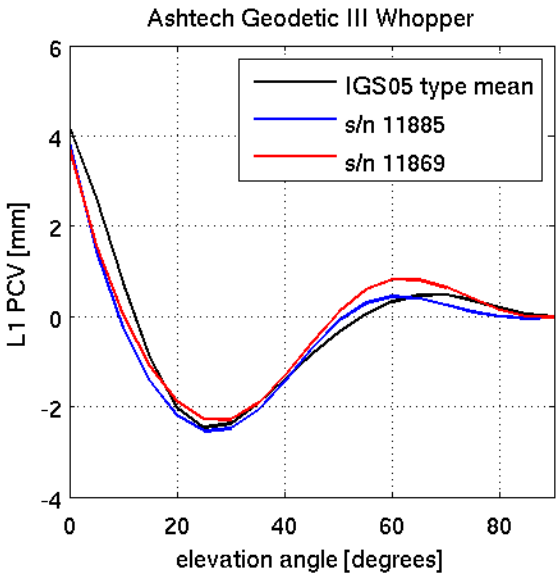

Figure 6: Elevation-only PCVs, GPS L1 frequency, for the Ashtech Geodetic III "Whopper" antenna. The two serial numbers calibrated (11885, 11869) are in close agreement with the IGS type mean for this antenna.

Table 2: NGS PCO solution for two different serial numbers of Ashtech Geodetic III "Whopper" antennas, compared to IGS05 type mean values.

(mm)	North	East	Up
IGS	-1.67	-0.47	69.48
11885	-1.22	0.22	69.13
11869	-1.40	0.23	69.17

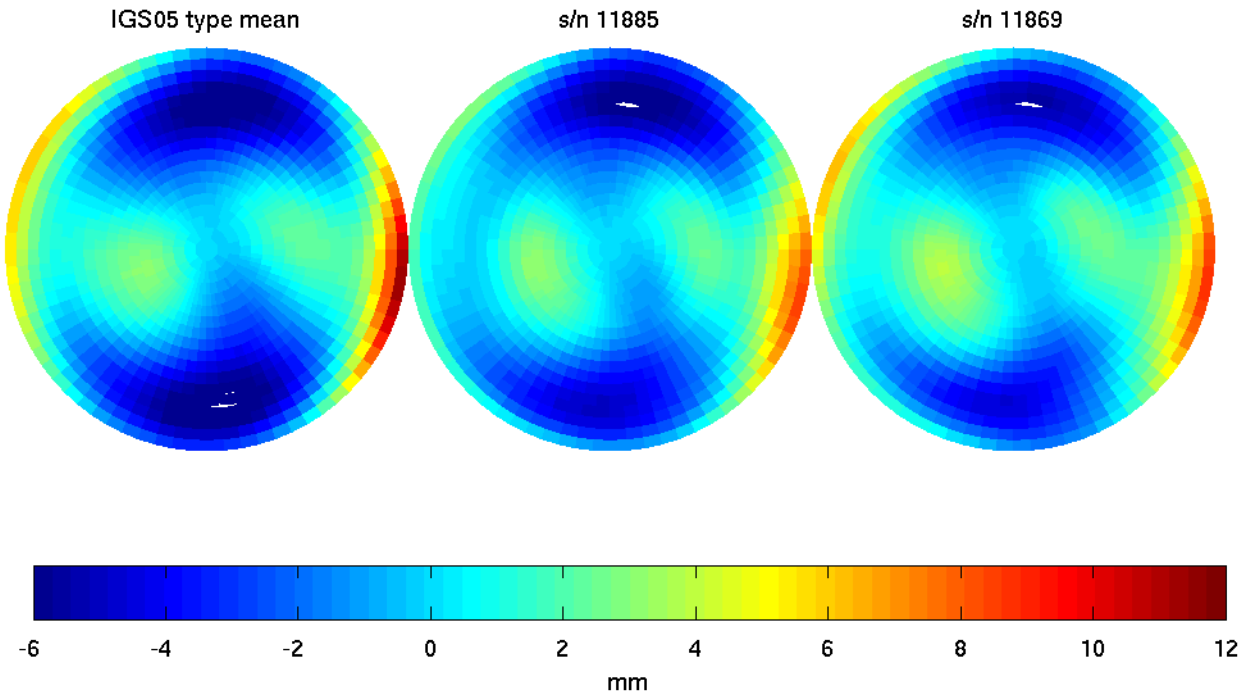

Figure 7: L1 PCVs for Ashtech Geodetic III "Whopper" antennas. The individual calibrations (center and right plots) show the same number and location of lobes as the IGS type mean (left-most plot). Color scale is given in mm.

NGS CALIBRATION SERVICES

All type mean antenna phase center values computed by the NGS facility will be publicly available and distributed via the Internet at http://www.ngs.noaa.gov/ANTCAL. Up until now, NGS calibrations have been distributed exclusively in the NGS format (http://www.ngs.noaa.gov/ANTCAL/format.txt). Although this format is limited to elevation-only PCV, the format is still in wide use for a variety of common GNSS processing software. To support both elevation- and azimuthal-dependence of PCV, final absolute APC values will also be distributed in the ANTEX format (ftp://igscb.jpl.nasa.gov/igscb/station/general/antex14.txt). Although NGS plans to conduct only absolute calibrations in the future, we note that absolute calibrations can be easily converted to relative calibrations [10] to suit GNSS analysis software.

The NGS absolute calibration facility was built to serve traditional NGS constituents such as the surveying and geodesy communities; however calibration services are open and available to all GNSS users as the calibration schedule permits. NGS is currently creating a calibration policy document to describe the calibration process, eligibility of antennas for calibration by NGS, and conditions for individual vs. type mean calibrations. The policy will soon be available via the ANTCAL URL given above. Calibration services will be no cost; the only expense for users and companies submitting antennas will be forward and return shipping. Although NGS will emphasize type mean calibration of previously uncalibrated antenna models, research-grade and one-off antennas will be eligible as the schedule permits.

NGS is concurrently developing a new web interface and related products to better serve our calibration customers. To submit an antenna or antenna group for calibration, users will fill out a web form with information about their antenna, including an engineering diagram of the antenna. This web form will submit the request to the NGS antenna calibration tracking system. This system will send automated emails to the customer at different stages in the calibration process and will streamline communications between the customer and NGS Calibration Services.

PROJECTIONS AND FUTURE WORK

The NGS absolute calibration system will soon be ready for full-time operations. Before accepting new antennas for calibration, NGS must complete work with the IGS Antenna Working Group to validate our results and ensure that NGS calibrations will be compatible with absolute calibrations computed by other facilities. Once NGS-IGS coordination is complete, the calibration submission web form will become active and absolute calibrations will being appearing alongside (but not

replacing) the relative calibration values at http://www.ngs.noaa.gov/ANTCAL.

Future work includes several refinements that must be made to enable calibration of all GNSS antennas. First, the current PTU weight limitations (max load of ~ 30 pounds when using 10 cm extension) prevent calibration of heavy antenna+radome+mount combinations. Also, as each GLONASS satellite has its own carrier frequency with a slight offset from the center frequency, we must explore the possibility that each GLONASS satellite will require its own calibration. Finally, the current requirement of a common clock input prevents calibration of integrated antenna-receiver units which do not accept an external clock input. Future work will include alternative solution methods which do not require a common clock at the reference and test antennas.

ACKNOWLEDGMENTS

The authors would like to thank Charles Geoghegan for his unfailing and expert administration of the NGS Corbin calibration facility. We also thank Dennis Lokken for calibration operations, Jaya Neti, Hong Chen, and David Geitka for website and web tools development, Steven Breidenbach, and Kendall Fancher for calibration site modification, measurements, and facility maintenance, Jarir Saleh for assistance with the spherical harmonic implementation, Heeyul Han for coding assistance, and Frank Marion for equipment management. Comments from Stephen Hilla and Mark Schenewerk strengthened the manuscript.

REFERENCES

[1] Mader GL (1999) GPS antenna calibration at the National Geodetic Survey, GPS Solutions 3(1):50–58, doi: 10.1007/PL00012780

[2] Wubbena G, M Schmitz, G Boettcher, C Schumann (2006) Absolute GNSS Antenna Calibration with a Robot: Repeatability of Phase Variations, Calibration of GLONASS and Determination of Carrier-to-Noise Pattern, proceedings of the IGS Workshop, May 8-12, ESOC, Darmstadt, Germany.

[3] Becker M, P Zeimetz, E Schönemann (2010) Anechoic chamber calibrations of phase center variations for new and existing GNSS signals and potential impacts in IGS processing, presentation at the IGS Workshop, 28 June - 2 July 2010, Newcastle upon Tyne, England.

[4] Schmid R, M Rothacher, D Thaller, P Steigenberger (2005) Absolute phase center corrections of satellite and receiver antennas: impact on global GPS solutions and estimation of azimuthal phase center variations of the satellite, GPS Solutions 9(4):283–293, doi: 10.1007/s10291-005-0134-x

[5] Zhu SY, F-H Massmann, Y Yu, C Reigber (2003) Satellite antenna phase center offsets and scale errors in GPS solutions, Journal of Geodesy 76:668–672, doi: 10.1007/s00190-002-0294-1

[6] Hatanaka Y, M Sawada, A Horita, M Kusaka (2001) Calibration of antenna-radome and monument-multipath effect of GEONET—Part 1: Measurement of phase characteristics, Earth Planets Space, 53, 13–21.

[7] Braun J, B Stephens, O Ruud, C Meertens (1997) The effect of antenna covers on GPS baseline solutions. UNAVCO report, University NAVSTAR Consortium, Boulder (available at http://facility.unavco.org/science_tech/dev_test/publications/dome_report/domeX5Freport-1.html)

[8] Bilich A, KM Larson (2007) Mapping the GPS multipath environment using the signal-to-noise ratio (SNR), Radio Science, 42, RS6003, doi:10.1029/2007RS003652.

[9] Wu JT, SC Wu, GA Hajj, WI Bertiger, SM Lichten (1993) Effects of antenna orientation on GPS carrier phase, Manuscripta Geodaetica 18, pp. 91-98.

[10] Schmid R, G Mader, T Herring (2005) From relative to absolute antenna phase center corrections, in Proceedings of the 2004 IGS Workshop and Symposium, Bern, pp 209–219